RESEARCH ARTICLE

Structural heterogeneity predicts ecological resistance and resilience to wildfire in arid shrublands

Andrii Zaiats · Megan E. Cattau · David S. Pilliod · Rongsong Liu · Patricia Kaye T. Dumandan · Ahmad Hojatimalekshah · Donna M. Delparte · T. Trevor Caughlin

Abstract

Context Dynamic feedbacks between physical structure and ecological function drive ecosystem productivity, resilience, and biodiversity maintenance. Detailed maps of canopy structure enable comprehensive evaluations of structure–function relationships. However, these relationships are scale-dependent, and identifying relevant spatial scales to link structure to function remains challenging.

Objectives We identified optimal scales to relate structure heterogeneity to ecological resistance, measured as the impacts of wildfire on canopy structure, and ecological resilience, measured as native shrub recruitment. We

further investigated whether structural heterogeneity can aid spatial predictions of shrub recruitment.

Methods Using high-resolution imagery from unoccupied aerial systems (UAS), we mapped structural heterogeneity across ten semi-arid landscapes, undergoing a disturbance-mediated regime shift from native shrubland to dominance by invasive annual grasses. We then applied wavelet analysis to decompose structural heterogeneity into discrete scales and related these scales to ecological metrics of resilience and resistance.

Results We found strong indicators of scale dependence in the tested relationships. Wildfire effects were most prominent at a single scale of structural heterogeneity (2.34 m), while the abundance of shrub recruits was sensitive to structural heterogeneity at a range of scales, from 0.07 – 2.34 m. Structural heterogeneity enabled out-of-site predictions of shrub recruitment ($R^2 = 0.55$). The best-performing predictive model included structural heterogeneity metrics across multiple scales.

Conclusions Our results demonstrate that identifying structure–function relationships requires analyses that explicitly account for spatial scale. As high-resolution imagery enables spatially extensive maps of canopy heterogeneity, models for scale dependence will aid our understanding of resilience mechanisms in imperiled arid ecosystems.

A. Zaiats · M. E. Cattau · A. Hojatimalekshah · T. T. Caughlin (✉)
Boise State University, Boise, ID, USA
e-mail: trevorcaughlin@boisestate.edu

D. S. Pilliod
U.S. Geological Survey, Forest and Rangeland Ecosystem Science Center, Boise, ID, USA

R. Liu
University of Wyoming, Laramie, WY, USA

P. K. T. Dumandan
University of Florida, Gainesville, FL, USA

D. M. Delparte
Idaho State University, Pocatello, ID, USA

Introduction

The concepts of ecological resistance and resilience provide insight into how ecosystems respond to disturbance in an era of unprecedented anthropogenic change (Chambers et al. 2014). However, identifying resistance and resilience in ecological data remains a long-standing challenge. Structural heterogeneity, including the spatial pattern of plant locations, its geometry in space, and functional diversity, provides a metric of ecosystem structure with broad relevance for post-disturbance recovery (Atkins et al. 2018; Ilangakoon et al. 2018; Walter et al. 2021; Lines et al. 2022). Heterogeneity generated by spatial variability in vegetation canopy and canopy gaps (interspaces) dictates soil erosion, snow distribution, and wildlife habitat (Webb et al. 2021; Johnson et al. 2021; Hojatimalekshah et al. 2023). Structural heterogeneity also determines impacts of disturbance, including wildfire severity (Koontz et al. 2020), and establishes trajectories of post-disturbance recovery (Fernández-Guisuraga et al. 2022). Utilizing structural heterogeneity to understand structure–function relationships will enhance our capacity to apply concepts of ecological resilience and resistance to conservation (Nimmo et al. 2015).

Structural heterogeneity can provide a barometer of ecological change with relevance across many systems (LaRue et al. 2019). For example, woody encroachment into grasslands and the degradation of shrublands by annual grass invasion both represent ongoing global ecosystem transformations characterized by loss of structural heterogeneity (Davies et al. 2011; Maestre et al. 2016). Across these ecosystem transformations, vegetation structure reflects state transitions and directions of change, including critical tipping points and recovery potential (Suding et al. 2004; Chambers et al. 2014). Nevertheless, the descriptors of spatial structure change across scales, complicating general rules for structure–function relationships (Levin 1992; Wu 2004; Maestre et al. 2016; Ilangakoon et al. 2021). Scale-dependent ecological processes, including disturbance and recovery, often result in divergent structural outcomes (Standish et al. 2014) because disturbance factors impact vegetation structure at specific spatial, temporal, and biological scales (Hobbs and Huenneke 1992; Buma and Wessman 2012; Atkins et al. 2020; Spake et al. 2022). Fulfilling the promise of structural data to advance ecological theory and aid land management will require defining scale-specific structural

patterns relative to disturbance effects (Chuang et al. 2018; Roberts et al. 2021).

While recent advances in remote sensing have enabled detailed maps of structural heterogeneity across large spatial extents (Getzin et al. 2014; Spiers et al. 2021; Lines et al. 2022), identifying scale-dependent ecological patterns from high-resolution data remains challenging. One solution is mathematical techniques that use wavelet transformation to quantify scale-dependence by decomposing variability in the data into discrete or continuous scales. In other words, wavelet transformation reduces complex spatial patterns into different components, each representing a unique scale. Wavelet analysis is widely used in fields such as signal processing, image analysis, and data compression, where understanding patterns at different levels of detail is important. In ecology, wavelet analysis can identify distinct scale-dependent patterns that are linked to spatial processes, such as seed dispersal and competition (Detto and Muller-Landau 2013). Applications of wavelet analysis in forestry have revealed scale-specific patterns in canopy heterogeneity related to disturbance-mediated ecosystem functions (Bradshaw and Spies 1992; Detto and Muller-Landau 2013). These analytical approaches can be powerful when management goals are explicitly defined in terms of structural complexity (Fahey et al. 2018; Seidel et al. 2019; Willim et al. 2020). As spatially extensive high-resolution data become increasingly available, wavelet analysis presents a promising way to extract scale-specific and ecologically relevant information from maps of canopy structure.

Drylands represent an ecosystem with an urgent need for the information that maps of structural heterogeneity could provide. Drylands are globally important yet vulnerable ecosystems where changes in structural heterogeneity often indicate state transitions (Maestre et al. 2021; Roberts et al. 2021). Anthropogenic threats to dryland ecosystems demand understanding the drivers of ecosystem resilience (Maestre et al. 2016; Berdugo et al. 2022). The Great Basin of the Western US exemplifies a threatened dryland ecosystem, where native shrublands are threatened by changing fire regimes, invasive species, and land use change (Davies et al. 2011; Pilliod et al. 2021). These disparate threats all result in changes in structural heterogeneity. Patchy shrub cover characterizes intact shrubland ecosystems in the region with clumps of native plants and interspaces dominated by soil biocrust. Novel wildfire regimes reduce structural heterogeneity in these patchy

ecosystems, decreasing shrub cover and expanding monocultures of invasive annual grasses (Ellsworth et al. 2020). Changes in the structural heterogeneity in shrublands can also result from woody encroachment, which reduces interspaces between shrubs with corresponding declines in ecosystem function (Pyke et al. 2015). These examples demonstrate how structural heterogeneity directly relates to ecological resilience in dryland ecosystems, including the Great Basin (Reinhardt et al. 2020; Pilliod et al. 2021).

We investigated the impacts of wildfire disturbance on structural heterogeneity and the relationship between recovery and structural heterogeneity in post-wildfire landscapes of the Great Basin. Ecological resistance to wildfire in the region, including where remnant shrub patches will persist, is spatially variable and not well understood (Applestein et al. 2022). After wildfire disturbance, native shrub recruitment is a crucial component of ecosystem resilience, representing the re-establishment of foundational plant species (Capdevila et al. 2020). Nevertheless, determinants of shrub recruitment are scale-dependent and remain challenging to predict (Germino et al. 2018a). Our study has two complementary objectives: exploring relevant ecological scales of heterogeneity after disturbance and testing how structural heterogeneity across scales predicts shrub recruitment. Using spatial data from ten post-fire landscapes, we ask the following questions: (i) What scales of structural heterogeneity best capture the impact of wildfire disturbance? (ii) What scales of structural heterogeneity are most sensitive to recovery, measured as the abundance of shrub recruits? As land management in the region increasingly relies on spatial decision-making (Meinke et al. 2009; Pilliod et al. 2021; Duchardt et al. 2021; Zaiats et al. 2023), we also determined how maps of structural heterogeneity can predict recovery by asking: (iii) Does a scale-explicit approach to analyzing structural heterogeneity enable out-of-site predictions of native shrub recruitment?

Methods

Overview

To answer our research questions, we used a combined dataset of unoccupied aerial systems (UAS) surveys and field observations in the Northern Great Basin. We surveyed ten sites with a consumer-grade UAS along the edge of a wildfire line, followed by extensive, randomized ground surveys of shrub abundance. We mapped all shrubs within 729 plots of 78.5 m^2 (circular shape with 5 m radius, Fig. 1) using a high-precision GPS system and stratified the shrubs into recruit (< 0.25 m) and adult (> 0.25 m) categories. Surveys resulted in 17 ha of high-resolution aerial imagery (< 2 cm/pixel ground sampling distance) and $> 10{,}000$ mapped shrub recruits. Next, we quantified the structural heterogeneity within each surveyed plot using a UAS-derived canopy height model and a discrete wavelet transform (DWT), which summarizes differences between neighboring pixels at a range of scales (i.e., grain sizes, Fig. 2). To answer questions 1 and 2, we used generalized linear models (GLMs) to quantify heterogeneity-wildfire and recruitment-heterogeneity relationships. To address question 3, we used GLMs and out-of-site cross-validation to quantify how well structural heterogeneity at different scales can predict recruitment at sites not used as training data.

Field surveys

Our research took place in southwestern Idaho, USA, in a cold semi-arid steppe with characteristic shrub vegetation cover. We selected field sites to include a range of elevation and time since wildfire site conditions (Table S1). We surveyed each site with the same sampling design: positioning approximately half of the rectangular footprint in intact shrubland, and the other half in an area previously burnt in a wildfire (Fig. 1). The previously burnt areas were intended to capture various states of post-disturbance recovery, ranging from 7 to 26 years since a wildfire event. To obtain the wildfire boundaries, we used a wildfire database (Welty and Jeffries 2021). We further refined the wildfire boundaries within our sites by hand-digitizing the abrupt change in shrub cover using the Google Earth historic imagery, corresponding to the year as close as possible after the wildfire event.

We randomly distributed 78.5 m^2 circular plots across the burnt and unburnt parts of the sites, placing between 49 to 97 plots per site. This design allowed for a representative sample of the references and disturbed vegetation states (White and Walker 1997). Because our sites spanned a wide range of
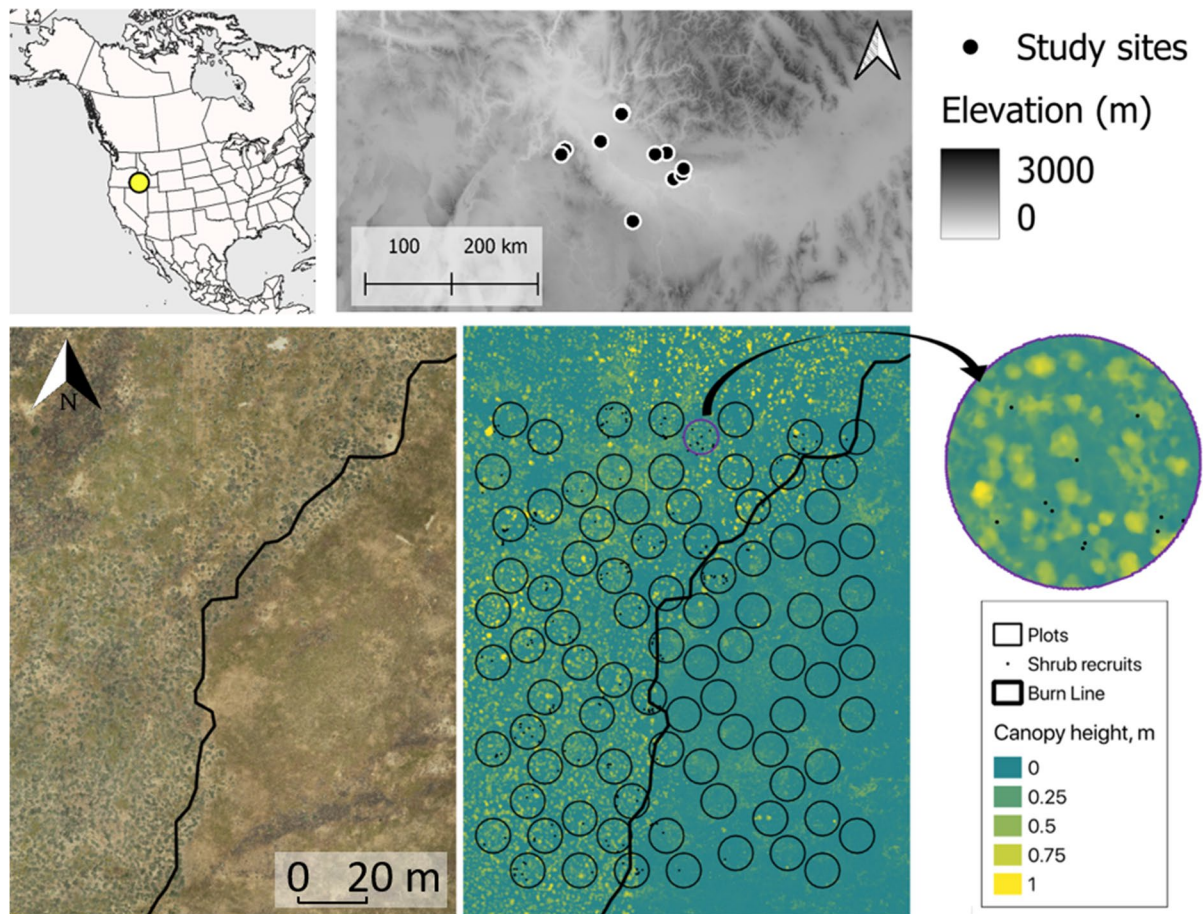
Fig. 1 The sampling design of UAS surveys and ground observations on an example of Cold wildfire site (2007) in SW Idaho, USA. The yellow dot on the map of North America indicates the location of our study region. The top right panel displays the location of our study landscapes relative to regional elevation. The true color image (bottom left) shows contrasts between the burnt and unburnt parts of the landscape, with predominantly shrub-less vegetation in the burnt section. The same area visualized as vegetation canopy height (bottom right) shows the distribution of field plots (hollow circles) and the locations of exhaustively mapped shrub recruits within the plots (black dots)

environmental conditions, each site had a different species composition, including the predominant species of canopy formation. In proportional representation across our field sites, approximately 75% of the data were represented by *Artemisia tridentata* (big sagebrush), 17% by *Artemisia arbuscula* (low sagebrush), 1–2% by *Chrysothamnus viscidiflorus* (yellow rabbitbrush), *Ericameria nauseosa* (rubber rabbitbrush), *Purshia tridentata* (antelope bitterbrush), and < 1% by *Eriogonum sphaerocephalum* (rock buckwheat), *Ribes aureum* (golden currant) and *Rosa woodsia* (Wood's rose). Within each 78.5 m² circular plot, we exhaustively mapped all shrubs by placing the GPS unit in the middle of the shrub crown. We

used a survey-grade RTK GPS unit (Topcon HiPer V, Topcon Positioning Systems Inc., Livermore, CA, USA) to collect geospatial data with ~ 0.02 m accuracy (Rayburn et al. 2011). Each plant was assigned a binary index to indicate whether the plant was above or below the 0.25 m maximum height threshold. We considered plants below the 0.25 m height threshold as recruits. Shrubs below 0.25 m tend to have lower probabilities of survival and fecundity, characteristic of juvenile plants (Shriver et al. 2019). Once the geospatial field data were collected, a post-processing correction was necessary to reduce the positioning errors. We used Online Positioning User Service (OPUS) and the proprietary software *MagnetTools*

Fig. 2 Raster plots visualizing vegetation structure through the canopy height model (left column) and spatial patterns of structural heterogeneity using discrete wavelet decomposition (DWT) with Haar wavelet filter applied to the same sections of the canopy height model (right column). The DWT disentangles the contribution of variance at different scales to spatial patterns in data. When the DWT is applied to a canopy height model, component scales represent structural heterogeneity
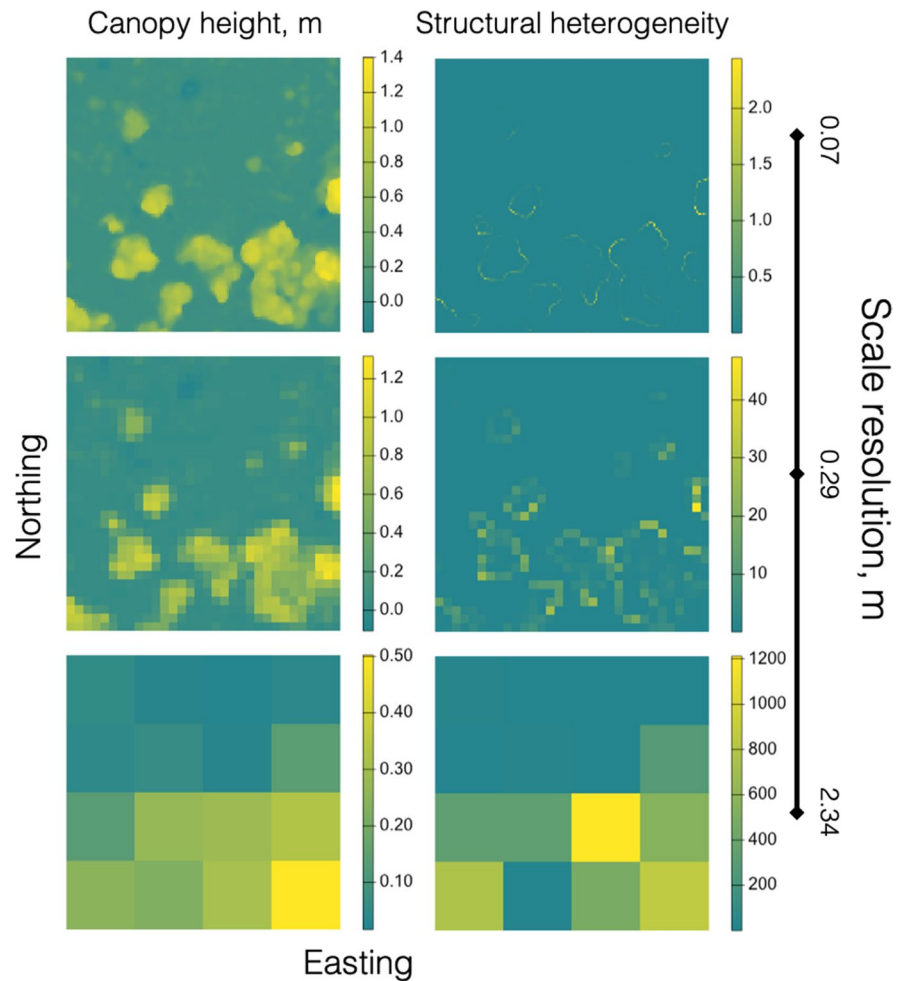
(Topcon Positioning Systems Inc., Livermore, CA, USA) to correct the data points.

UAS data

We used unoccupied aerial systems (UAS) data to obtain spatially explicit structural metrics of the vegetation (Marie et al. 2023a, a, b, c, d, e, f, g). Each UAS survey was conducted with a consumer-grade DJI Mavic 2 Pro (SZ DJI Technology Co., Ltd., Nanshan, Shenzhen, China). Briefly, all surveys had comparable flight parameters: 44 m flight altitude, cross grid flight with 20° yaw offset combined with nadir + 5° offset camera angle for the second grid path, 2 m/s flight speed, 75/80 forward and side overlap, with the flight times between 10 am and 3 pm under uniform lighting conditions (see Marie et al. 2023a-h for more details). The flight parameters resulted in high-resolution imagery with < 2 cm/pixel ground sampling distance (GSD). Each UAS product included a raster and a point cloud representing the digital surface model (DSM), which tracks vegetation and topographic changes over the landscape. We restricted our focus to the structural characteristics composed only of the vegetation component and removed the topographic variation from the DSM by subtracting the digital terrain model (DTM).

We generated the DTM by applying existing software tools to fine-tune the DSM, using open-source tools *CloudCompare* and 'lidR' package (Girardeau-Montaut 2016; Zhang et al. 2016; Roussel et al. 2020), https://github.com/andriizayac/uas_data_preprocess). As an initial step, we applied Cloth Simulation Filter (Zhang et al. 2016) to roughly separate vegetation from ground. Next, we used Statistical Outlier Removal (SOR) to filter remaining ("floating")

clusters of points missed by CSF. Because CSF and SOR may not accurately separate ground from vegetation along the margins of shrub crowns or near small shrub recruits, we relied on surface curvature to further refine the terrain model. Specifically, we used two radii for calculating the curvatures and threshold filtering to capture the surfaces characterized by high curvature including margins of crowns and small vegetation features (e.g., recruits). We hand-adjusted the input values for the CSF and curvature filtering and thresholding based on each landscape scene to acquire the most accurate digital terrain and canopy height models. We used the resultant canopy height model (CHM) as an input to quantify vegetation structure.

Structural heterogeneity

We used Discrete Wavelet Transform (DWT) to quantify structural heterogeneity from the CHM and decompose it into discrete scales of variability. We use the term "scale" to refer to comparisons between different levels of aggregated pixels, following previous work that has applied wavelet transform to spatial data (Bradshaw and Spies 1992; Detto and Muller-Landau 2013). Wavelet transform decomposes a signal (*e.g.*, canopy height) into low- to high-frequency changes (Bradshaw and Spies 1992). For example, low-frequency canopy changes may correspond to the presence and arrangement of large plants, while high-frequency canopy changes may reflect branches or seedlings. Wavelet transform has broad applications in ecology, including understanding scale-dependence in forest spatial structure and community dynamics (Bradshaw and Spies 1992; Keitt and Fischer 2006; Walter et al. 2017). We used the 'wavethresh' package (Nason and Nason 2016) to decompose spatial variability in the CHM into discrete scales of variation using a multi-resolution representation of the DWT (65, p. 70):

$$CHM_M = CHM_{m_0} + \sum_{m=1}^{m_0} \boldsymbol{D}_m \tag{1}$$

Here, Eq. 1 shows the original canopy height model (CHM_M) as a sum of a smoothed canopy at scale m_0, CHM_{m_0}, and detail coefficients $\boldsymbol{D}_m$ at scales

from the finest to the coarsest level of smoothing, m_0. Scale M was the original resolution of the CHMs, while $m = 1$ and $m = 9$ corresponded to the finest and coarsest levels of the DWT, respectively. We chose m_0, the level of CHM smoothing in DWT, at the resolution 18.72 m as it exceeded the extent of our field plots. An overarching objective of our study is to identify which scales are most informative for quantifying ecological resilience and resistance. The spatially explicit, two-dimensional array $\boldsymbol{D}_m$ is the sum of horizontal, vertical, and diagonal difference coefficients, $\boldsymbol{D}_m = \boldsymbol{D}^h_m + \boldsymbol{D}^v_m + \boldsymbol{D}^d_m$ (Fig. 3; 65, p. 127). Multiple options exist for the choice of the wavelet function with subtle differences in the inferred patterns (Keitt and Fischer 2006). We chose the Haar wavelet in DWT to highlight the vertical changes in canopy structure, *i.e.*, plant margins, as canopy features representing structural heterogeneity, and to mitigate boundary artifacts in the transform due to the local support of the Haar wavelet (Bradshaw and Spies 1992; Addison 2017).

We quantify structural heterogeneity for each plot (*i*) at the scale (*m*) as a sum of squared Haar difference (detail) coefficients, $Heterogeneity_{m,i}(\boldsymbol{x}, \boldsymbol{y}) = \sum_{j=1}^{n} \boldsymbol{D}^2_s(x_j, y_j)$, where vectors ($\mathbf{x}$, $\mathbf{y}$) delineate the 78.5 m² buffer area of a 5 m radius from plot center, and *n* indicates all pixels (x_j, y_j) within the plot boundaries. Difference coefficients characterize changes in the canopy structure by comparing the canopy height values at neighboring pixels. For example, a high wavelet coefficient at scale (*m*) would correspond to four very different pixels at a finer scale (*m*-1). The finest scale, *M*, corresponds to the original raster input of the canopy height model. Note that the index *m* is a discrete integer that corresponds to nine different scales from 0.04 to 9.36 m.

Data analysis

Wavelet transformation of the CHM resulted in characteristic variability of the canopy across nine scales. We ran three separate analyses designed to answer our three primary questions. To answer our first question and identify the optimal scale to detect wildfire effects, we ran the following set of linear mixed-effect regressions:

Fig. 3 The scale-dependent effect sizes in (**a**) structural heterogeneity-wildfire and (**b**) recruitment-heterogeneity relationships in Great Basin shrublands. The x-axis in (a-b) corresponds to structural heterogeneity measured at distinct scales (meters). The effect of wildfires (**a**) indicates changes in structural heterogeneity relative to intact vegetation (Fig. 1). The effect size shows the decline in canopy structural heterogeneity in units of squared differences between neighboring pixels. The results of the sparse model (**b**) show the effects of different scales of heterogeneity on recruit abundance, where the effect size indicates the expected change in log-recruit abundance under an increase of predictors by one SD of log-structural heterogeneity. The points indicate the means, and the error bars correspond to 95% CI of the posterior distribution
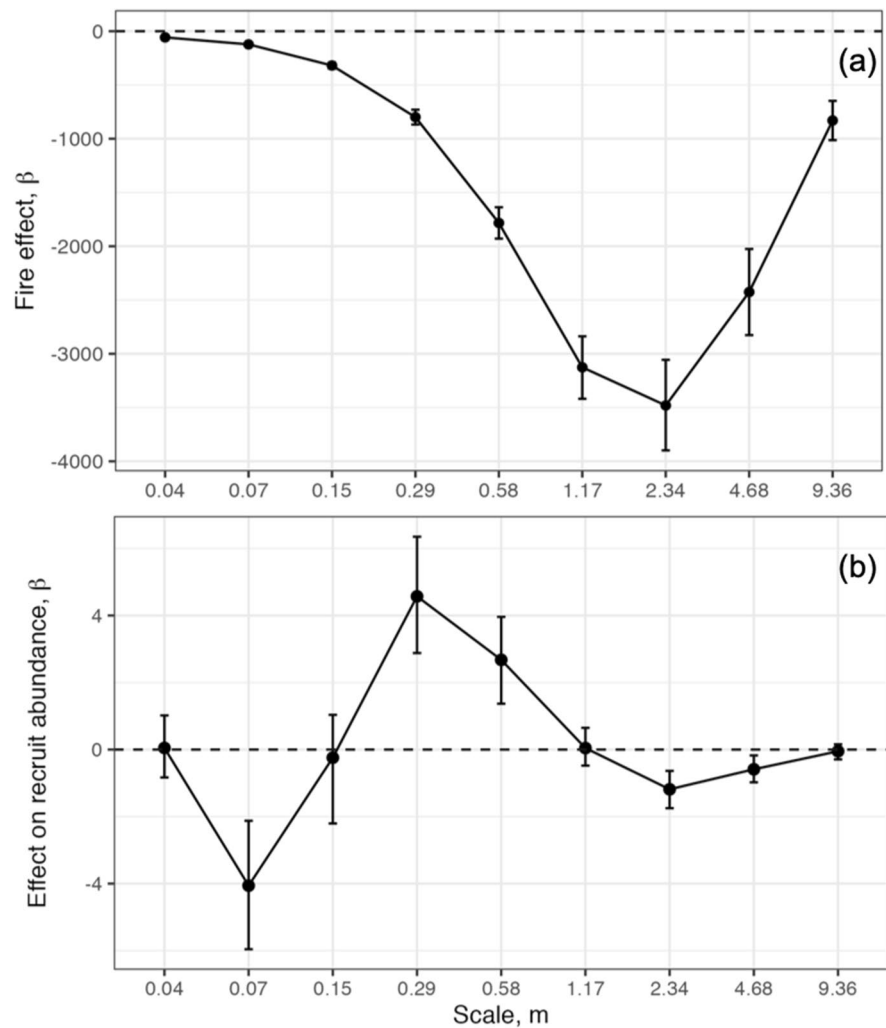
$$H^{(m)} \sim N\left(\beta_{0|site}^{(m)} + \beta_1^{(m)} wildfire, \sigma \right) \qquad (2)$$

Differences between the estimated $\beta_1^{(m)}$ across models (m) indicate that heterogeneity at each scale m, $H^{(m)}$, has varying degrees of sensitivity to wildfire effects. The wildfire effect was quantified using a binary variable indicating whether the plot was within the burnt or the reference, unburnt area, where $\beta_1^{(m)}$ is vector of two coefficients for each model corresponding to (m) scale. We used site as a random effect to account for baseline site differences in heterogeneity. This random effect reflects the myriad factors that influence fire severity in sagebrush steppe landscapes (Chambers et al. 2014). To address our second question and identify optimal scales of heterogeneity for

shrub recruitment, we ran a sparse linear regression with negative binomial error distribution and a regularizing horseshoe prior (Piironen and Vehtari 2017):

$$R \sim NegBinom\left(\exp(\beta_0 + H \cdot \beta_1), \phi \right) \qquad (3)$$

where H is a matrix of nine log-transformed heterogeneity predictors ($m = 1, 2, \ldots, 9$), and β_1 is a vector of nine coefficients quantifying the effect size of each heterogeneity scale on the recruit abundance. We used a strong regularizing horseshoe prior with maximum local and global shrinkage that allowed for model convergence (df = 1, df$_{global}$ = 2), with the ratio of expected non-zero to zero coefficients set to 0.01 (Bürkner 2017; Piironen and Vehtari 2017; Simler-Williamson et al. 2022). Similar sparse models have

been successfully applied to select relevant scale of wavelet coefficients through the shrinkage variable selection (Zhao et al. 2012, 2015).

In question three, we focused on quantifying how well structural heterogeneity can predict recruitment. We implemented two predictive models using negative binomial generalized linear models. First, we tested an additive effect of scale-specific structural heterogeneity, starting from the coarsest scale (9.36 m) of heterogeneity as a single predictor and adding one other scale at the next, finer resolution per model.

$$R \sim NegBinom\Big(\exp(\beta_0^{(m)} + \beta_1^{(m)} elevation + \boldsymbol{H}_{[9:m]}\boldsymbol{\beta}_2^{(m)}), \phi\Big), form = 9, 8, \ldots, 1 \tag{4}$$

As a result, we obtained a set of models with a varying number of coefficients in $\boldsymbol{\beta}_2^{(m)}$, $(1:m)$, corresponding to a subset of columns in matrix $\boldsymbol{H}_{[9:\boldsymbol{m}]}$. We included elevation in our model to account for the site differences as elevation is a key determinant of sagebrush recruitment in heterogeneous landscapes (Germino et al. 2018b). The second predictive analysis paralleled the structure of *Eq.* 4, but included only one scale of structural heterogeneity per model (*Eq.* 5). Including a single scale of heterogeneity at a time directly compares the predictive power of each scale relative to the others.

$$R \sim NegBinom\Big(\exp(\beta_0^{(m)} + \beta_1^{(m)} elevation + H_{[m]}\beta_2^{(m)}), \phi\Big), form = 9, 8, \ldots, 1 \tag{5}$$

For each model, we generated an R^2 metric of model fit and a predicted recruit abundance (Gelman et al. 2019). We then calculated the mean absolute error (MAE) following:

$$MAE = \frac{1}{N} \sum_{i=1}^{N} |y_i - \hat{y}_i|$$

where N is the number of field plots, y is the observed abundance data, and $\hat{y}$ is the predicted abundance of shrub recruits. We evaluated R^2 and MAE using k-fold cross-validation approach. Specifically, we split the dataset into 10 groups and withheld one group at a time from model fitting—the withheld group corresponded to all plots belonging to a single site.

We used 'brms' package and ran the linear models in the Bayesian framework with default priors, except the sparse models, where we used regularizing priors (Bürkner 2017). For all data manipulation and analysis we used *R* software v4.2.2 (R Core Team 2021), including 'tidyverse', 'sf', 'terra', 'ggplot2' packages (Wickham 2011; Pebesma 2018; Wickham et al. 2019; Hijmans et al. 2022).

Results

Structural heterogeneity and ecological resistance to wildfires

Relative to the unburnt vegetation, wildfires reduced structural heterogeneity in the burnt areas by 74% (95%CI: 59–87). This difference emerged across ten sites that differed considerably in elevation (867–1514 m), time-since-fire (7–26 years), average slope (1.7–23.4°), and wildfire severity (low-moderate). The magnitude of wildfire-related structural changes varied across scales. Our scale-explicit analysis identified a single optimal scale for detecting structural differences between burnt and unburnt areas (2.34 m; Fig. 3a), with weaker effects at both the finest (0.04 m) and coarsest (9.36 m) scales. There was high certainty that the 2.34 m scale best captured wildfire effects, including the probability of difference between posterior distributions for 2.34 m and all other scales > 0.99, except the 1.17 m scale, where the probability of difference was 0.87. This outcome highlights strong agreement between our disparate sites that 2.34 m provided an optimal scale to summarize structural heterogeneity for wildfire legacy.

Recruitment and structural heterogeneity

In contrast to the unimodal relationship between scales of structural heterogeneity and disturbance effects, ecosystem resilience, measured as the abundance of shrub recruits, was associated with structural heterogeneity across multiple scales (Fig. 3b). Across the nine scales of structural heterogeneity we tested, we found peak effect sizes at 0.07, 0.29, and 2.34 m, with decreased effect sizes for other scales. Effect sizes also indicate that heterogeneity from coarse to fine scales increases in magnitude, suggesting a stronger association between finer scale heterogeneity and recruit count.

Structural heterogeneity as a predictor of recruitment

Scale-explicit analyses of structural heterogeneity enabled spatial predictions of shrub recruits across post-fire landscapes. A combination of structural heterogeneity metrics from 9.36—0.07 m scales resulted in out-of-site Bayesian R^2 of 0.55 (95%CI: 0.47–0.62), with a mean absolute error (MAE) of 0.28 recruits m^{-2}. These metrics indicate that structure-from-motion data collected by UAS imagery can predict shrub recruitment at sites without available field data. When each scale of heterogeneity was tested as an individual predictor in a single model, the model with the greatest predictive power incorporated structural heterogeneity at the 0.29 m scale (Fig. 4b). At this resolution, pixel sizes derived from the canopy height model are likely bigger than an average shrub recruit. However, high heterogeneity at this resolution implies greater differences between neighboring pixels at the scale of 0.15 m, which could indicate a plant recruit. Scales of heterogeneity smaller or greater than 0.29 m individually predicted recruitment with similar or lesser accuracy.

The decomposition of total heterogeneity into discrete scales improved prediction accuracy compared to the baseline model, a model with a single predictor for total structural heterogeneity within each plot (*i.e.*, all nine scales added together). The model with total structural heterogeneity had an out-of-site predictive R^2 of 0.39 (95%CI: 0.34–0.44) and an MAE of 0.41 shrub recruits m^{-2}, a loss of R^2 at 0.16 and MAE at

0.13 shrubs m^{-2} compared to the model with multiple structural heterogeneity metrics. Because effect sizes for structural heterogeneity on recruitment varied across scales, including positive and negative effects (Fig. 3b), averaging across these scales results in a loss of information. This result suggests that different scales of heterogeneity contain different information related to ecological processes (Fig. 4a). When evaluating scales individually (best model R^2=0.43, MAE=0.32 shrubs m^{-2}; Fig. 4b), structural heterogeneity at the scale of 0.29 m resulted in lesser improvements over the total heterogeneity model.

Discussion

Mapping structural heterogeneity enables insights into ecosystem functions that determine ecological resistance and resilience (Koontz et al. 2020; Mahood et al. 2023). We found strong evidence for scale-dependent effects of structural heterogeneity on resistance and resilience to wildfires in a semi-arid ecosystem. Our approach highlights the importance of fundamental questions of scale in interpreting structural information (Levin 1992). An explicit approach to choosing spatial scales in data analysis will enhance the applied value of ecological models (Spake et al. 2021). We found that structural differences between burned and unburned areas were greatest at approximately the scale of adult shrubs. This indicates that a foundational component of sagebrush ecosystems has relatively low ecological resistance to wildfire. Our findings also reveal multi-scale impacts of structural heterogeneity on shrub recruitment, a starting point for understanding demographic mechanisms that underlie ecological resilience in our study system. Positioning scale-dependent effects of structural heterogeneity within existing management and theoretical frameworks will boost the capacity of remotely sensed data to provide ecological insight.

Structural heterogeneity and wildfires

Wildfires reduced structural heterogeneity across all scales (Fig. 3a). However, our models identified a single optimal scale where the relationship

Fig. 4 The line plot shows the importance of different scales of canopy structural heterogeneity for predicting shrub recruit abundance. Scales correspond to (**a**) a step-wise addition of finer resolutions starting from the finest level at 0.04 m, and (**b**) individual scales of structural variation with the rest of the scales removed. Solid black lines indicate the mean, while dotted black lines represent the 95% credibility interval of R^2 metric. Dashed gray lines correspond to the average mean absolute error (MAE, right y-axis). The solid horizontal lines show the predictive power of the base model, where all scales of structural heterogeneity were added together and used as a single predictor. The solid black horizontal line indicates the R^2 metric for the base model, while the dashed gray horizontal line indicates MAE for the base model
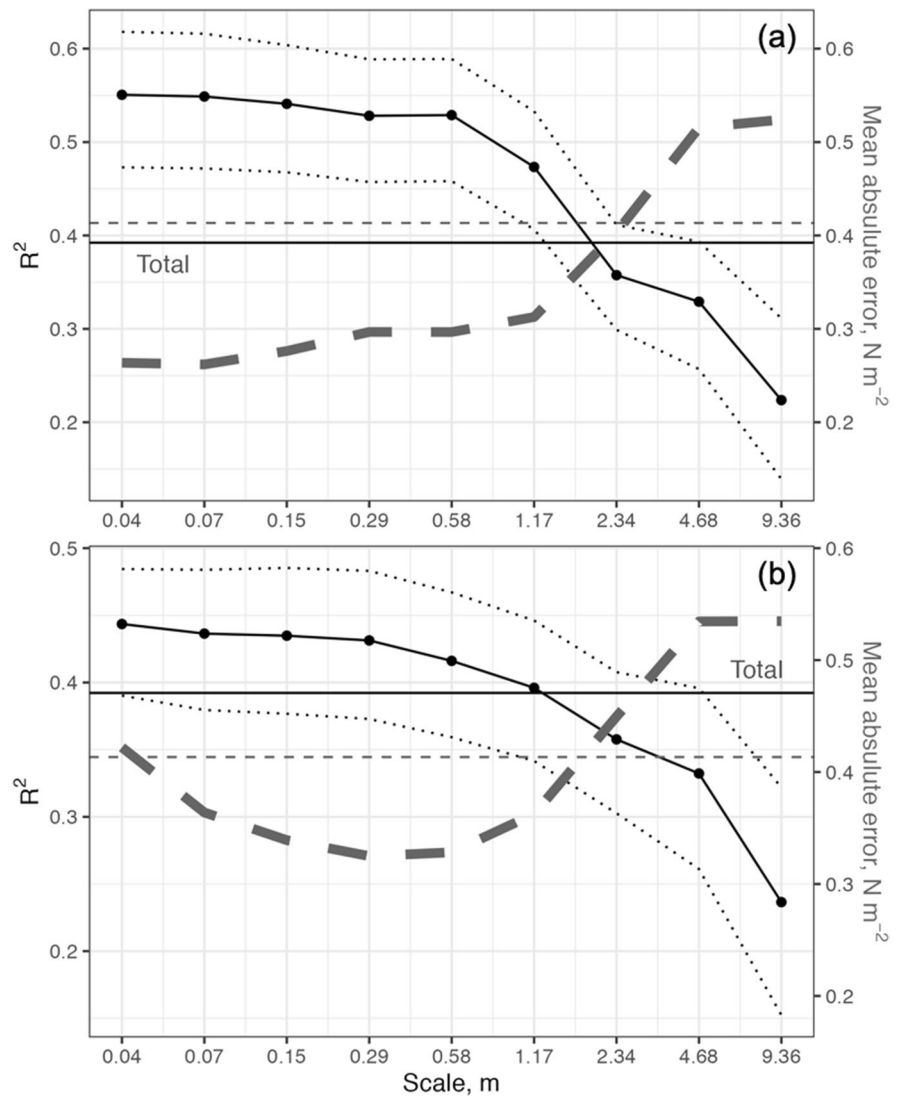
between structural heterogeneity and wildfire was strongest. The presence of a single optimal scale is consistent with previous evidence from forest ecosystems: pulse disturbances like wildfire may impose functionally similar effects on vegetation structure despite differences in site conditions, time since fire, and wildfire severity (Atkins et al. 2020). Wildfires in the Great Basin may equally remove large and small vegetation from the landscape (Miller et al. 2013; Requena-Mullor et al. 2019; Mahood et al. 2023), inherently erasing or modifying structural patterns across multiple scales. Post-disturbance heterogeneity across scales is unequal

and depends on vegetation properties. For example, in a forest ecosystem, the maximum individual tree complexity within a plot explains stand-level structural heterogeneity better than the sum of individual tree complexities (Seidel et al. 2019). In our study, the selected optimal scale (2.34 m) roughly captures a single large shrub and its boundaries, suggesting that patterns related to adult plants drive post-disturbance changes in structural heterogeneity. We hypothesize that the optimal scale of structural heterogeneity as an effect of wildfires may be related to the absence of at least one adult large shrub in burnt areas. These results suggest

that the best scale to aggregate canopy height models to represent structural heterogeneity may be proportional to the size of largest plant crowns in the landscape.

Identifying which scales respond most strongly to wildfire provides insight into which ecological components are least resistant to disturbance, for example, adult shrubs. Sagebrush shrublands may take 30 years or more to regenerate cover and height to pre-disturbance levels (Baker 2006; Ziegenhagen and Miller 2009). Our results show the potential for structural patterns to indicate remnant patches in sagebrush shrublands after wildfire.

Our analyses demonstrate how structural heterogeneity can provide insight into resistance to disturbance in dryland ecosystems. Heterogeneous vegetation cover, including shrubs, herbaceous plants, bare ground, and soil crusts (Davies et al. 2011; Condon and Pyke 2018), characterizes healthy shrublands of the Great Basin. In contrast to biomass or cover estimates that may not always be sensitive metrics of ecosystem change (Atkins et al. 2020), structural heterogeneity provides information about vegetation presence and its spatial arrangement, including quantitative estimates of shrub interspaces. The ~2 m scale we identify as a strong predictor of disturbance in our analyses likely quantifies the presence of foundational shrub species and characteristic canopy gaps in our study sites (Condon and Pyke 2018). In ecosystems where herbaceous species are the primary components of ecosystem structure with low patchiness, we expect to observe strong effects of disturbance at finer scales. Overall, our results demonstrate the overall value of structural heterogeneity and the importance of scale-explicit analytical approaches for quantifying resistance to disturbance.

Recruitment and structural heterogeneity

Our models suggest that multiple scale-specific processes drive structural heterogeneity associated with ecosystem resilience (Levin 1992; Maestre et al. 2016). We found evidence for both positive and negative relationships between recruitment and structural heterogeneity, depending on spatial scale. Structural heterogeneity increased recruitment at spatial scales from 0.29–0.58 m. Potential explanations for these positive relationships

include the presence of small canopy gaps that may facilitate shrub recruitment (Condon and Pyke 2018) or short-distance seed dispersal from nearby adult shrubs (Applestein et al. 2022). In contrast, we observed negative relationships between structural heterogeneity and recruitment at scales of 0.07 and 2.34 m. We hypothesize that competitive interactions may underlie these negative associations. The negative effect at the 2.34 m scale may point to competitive pressures from adult shrubs that limit favorable spaces and conditions for shrub recruits (Schwinning and Weiner 1998; Adler et al. 2010). Fine-scale heterogeneity (0.07 m) was also negatively associated with recruitment. The negative effect of structural heterogeneity on recruitment at fine scales may be due to competition with invasive annual grasses and forbs. Exotic vegetation creates adverse conditions for shrub recruitment by limiting shrub seed arrival or imposing high resource competition (Arkle et al. 2014, p. 20; Applestein and Germino 2022). Our results highlight the need for future studies that link structural heterogeneity to plant-plant interactions, including competition and facilitation between neighboring plants.

An alternate explanation for positive relationships between shrub recruitment and structural heterogeneity is that, at some scales, remote sensing imagery is detecting shrub canopies. The abundance of shrubs below 0.25 m likely contributes most to structural heterogeneity at scales of 0.29–0.58 m, where we found positive relationships recruitment and structural heterogeneity. Wavelet-based techniques for edge detection are heavily used in image analysis, with a demonstrated capacity to recognize plants in aerial imagery (Strand et al. 2007; Addison 2017). The delineation of plant edges using wavelet techniques directly corresponds to structural heterogeneity metrics, as plant edges create heterogeneity at specific scales. This scale-specific positive sensitivity of structural heterogeneity and recruit abundance suggests structural heterogeneity as a data source to detect and predict recruitment.

Structural heterogeneity as a predictor of recruitment

Our results emphasize how structural heterogeneity can be a powerful predictor of ecosystem function

(LaRue et al. 2019). Decomposing structural heterogeneity into specific scales boosts the ability of these metrics to predict ecologically relevant outcomes, particularly when multi-scale metrics are included in the same predictive model. Predictions of natural regeneration after disturbance, including recruitment, will aid decision-making on where to allocate limited resources for restoration (Barber et al. 2022).

We demonstrate how remotely sensed structural information can aid predictions of natural regeneration capacity. UAS, in particular, have potential for rapid deployment over large areas. While the extent of a single flight designed to collect ultra high-resolution imagery (< 1 cm), such as the RGB imagery used in this paper, may be less than the extent of land management units, we anticipate that multiple flights could sample entire landscapes. We have demonstrated the capacity of relatively inexpensive commercial UAS platforms to collect high-quality structural data, with relevance to ecological resilience and resistance. The ease of use of these platforms should facilitate multiple flights capable of capturing larger extents. Structure-for-motion algorithms enable extraction of structural data from relatively inexpensive commercial UAS platforms, including RGB-only sensors (Zahawi et al. 2015). The advance we have developed in this paper is to show that structural heterogeneity can accurately predict shrub recruitment without relying on site-specific training data. This approach is relatively simple compared to remote sensing workflows that apply machine learning algorithms to identify objects in imagery and classify them to species (e.g., Retallack et al. 2022). The most complex step in our workflow is developing a canopy height model, which may require site-specific fine-tuning. Fortunately, publicly-available workflows and open source software (e.g., CloudCompare; Girardeau-Montaut 2016) exist to aid with this step. Low-cost maps of structural heterogeneity could enable rapid assessments of ecological resilience, even for sites where no field data is available.

Expanding scale-explicit analyses to data sources with broader geographic extents, beyond the footprint of individual UAS flights, could aid regional conservation efforts. Potential data sources that could map structural heterogeneity across large areas include aerial lidar and satellite-borne radar sensors (Fernández-Guisuraga et al., *In press*). Structural heterogeneity measurements from these sensors could address region-wide conservation challenges, from tree encroachment to expansion of invasive annual grass monocultures (Pilliod et al. 2021; Smith et al. 2021). Scale-explicit analyses could also improve the spatial placement of restoration treatments by matching the scale of spatial patterns generated by management interventions (*e.g.*, seeding or fuel reduction treatments) to the scales of ecological outcomes (*e.g.*, recruitment limitation or fire extent and severity).

Conclusions

Feedback between ecosystem structure and function underlies ecosystem recovery after disturbance. We found that maps of canopy structural heterogeneity enabled us to quantify structure–function relationships during post-fire recovery in a semi-arid shrubland. Accounting for scale-dependence in these relationships was critical for ecological inference and prediction. Structural heterogeneity captured the impacts of wildfires across divergent landscapes, with the strongest effects at a single spatial scale. In contrast, native shrub recruitment, indicative of ecosystem functioning after succession, was related to structural heterogeneity across a range of scales. In practical applications, detecting optimal scales for monitoring disturbance effects and regeneration can guide future remote sensing efforts for natural resource management. Optimal scales of structural heterogeneity also show promise as a predictive tool to assess the recovery trajectories of degraded ecosystems. We conclude that the scale decomposition of vegetation structural information will likely be fruitful for future studies aiming to link ecosystem structure and function.

Data availability The UAS data used in the manuscript are publicly available and can be accessed from Marie et al. 2023a-h (full citations in the References section). Field data, processing and analysis R scripts will be published on the Zenodo digital repository.

Declarations

Competing interests The authors declare no competing interests.

References

Addison PS (2017) The illustrated wavelet transform handbook: introductory theory and applications in science, engineering, medicine and finance. CRC Press

Adler PB, Ellner SP, Levine JM (2010) Coexistence of perennial plants: an embarrassment of niches. Ecol Lett 13:1019–1029. https://doi.org/10.1111/j.1461-0248.2010.01496.x

Applestein C, Germino MJ (2022) Patterns of post-fire invasion of semiarid shrub-steppe reveals a diversity of invasion niches within an exotic annual grass community. Biol Invasions 24:741–759. https://doi.org/10.1007/s10530-021-02669-3

Applestein C, Caughlin TT, Germino MJ (2022) Post-fire seed dispersal of a wind-dispersed shrub declined with distance to seed source, yet had high levels of unexplained variation. AoB PLANTS 14:plac045. https://doi.org/10.1093/aobpla/plac045

Arkle RS, Pilliod DS, Hanser SE et al (2014) Quantifying restoration effectiveness using multi-scale habitat models:

implications for sage-grouse in the Great Basin. Ecosphere 5:art31. https://doi.org/10.1890/ES13-00278.1

Atkins JW, Bohrer G, Fahey RT et al (2018) Quantifying vegetation and canopy structural complexity from terrestrial LiDAR data using the forestr r package. Methods Ecol Evol 9:2057–2066. https://doi.org/10.1111/2041-210X.13061

Atkins JW, Bond-Lamberty B, Fahey RT et al (2020) Application of multidimensional structural characterization to detect and describe moderate forest disturbance. Ecosphere 11:e03156. https://doi.org/10.1002/ecs2.3156

Baker WL (2006) Fire and Restoration of Sagebrush Ecosystems. Wildl Soc Bull 34:177–185. https://doi.org/10.2193/0091-7648(2006)34[177:FAROSE]2.0.CO;2

Barber C, Graves SJ, Hall JS et al (2022) Species-level tree crown maps improve predictions of tree recruit abundance in a tropical landscape. Ecol Appl 32:e2585. https://doi.org/10.1002/eap.2585

Berdugo M, Gaitán JJ, Delgado-Baquerizo M et al (2022) Prevalence and drivers of abrupt vegetation shifts in global drylands. Proc Natl Acad Sci 119:e2123393119. https://doi.org/10.1073/pnas.2123393119

Bradshaw GA, Spies TA (1992) Characterizing Canopy Gap Structure in Forests Using Wavelet Analysis. J Ecol 80:205–215. https://doi.org/10.2307/2261007

Buma B, Wessman CA (2012) Differential species responses to compounded perturbations and implications for landscape heterogeneity and resilience. For Ecol Manage 266:25–33. https://doi.org/10.1016/j.foreco.2011.10.040

Bürkner P-C (2017) brms: An R package for Bayesian multilevel models using Stan. J Stat Softw 80:1–28

Capdevila P, Stott I, Beger M, Salguero-Gómez R (2020) Towards a Comparative Framework of Demographic Resilience. Trends Ecol Evol 35:776–786. https://doi.org/10.1016/j.tree.2020.05.001

Chambers JC, Miller RF, Board DI et al (2014) Resilience and Resistance of Sagebrush Ecosystems: Implications for State and Transition Models and Management Treatments. Rangel Ecol Manage 67:440–454. https://doi.org/10.2111/REM-D-13-00074.1

Chuang WC, Garmestani A, Eason TN et al (2018) Enhancing quantitative approaches for assessing community resilience. J Environ Manage 213:353–362. https://doi.org/10.1016/j.jenvman.2018.01.083

Condon LA, Pyke DA (2018) Fire and Grazing Influence Site Resistance to Bromus tectorum Through Their Effects on Shrub, Bunchgrass and Biocrust Communities in the Great Basin (USA). Ecosystems 21:1416–1431. https://doi.org/10.1007/s10021-018-0230-8

Davies KW, Boyd CS, Beck JL et al (2011) Saving the sagebrush sea: An ecosystem conservation plan for big sagebrush plant communities. Biol Cons 144:2573–2584. https://doi.org/10.1016/j.biocon.2011.07.016

Detto M, Muller-Landau HC (2013) Fitting Ecological Process Models to Spatial Patterns Using Scalewise Variances and Moment Equations. Am Nat 181:E68–E82. https://doi.org/10.1086/669678

Duchardt CJ, Monroe AP, Heinrichs JA et al (2021) Prioritizing restoration areas to conserve multiple sagebrush-associated wildlife species. Biol Cons 260:109212. https://doi.org/10.1016/j.biocon.2021.109212

Ellsworth LM, Kauffman JB, Reis SA et al (2020) Repeated fire altered succession and increased fire behavior in basin big sagebrush–native perennial grasslands. Ecosphere 11:e03124. https://doi.org/10.1002/ecs2.3124

Fahey RT, Alveshere BC, Burton JI et al (2018) Shifting conceptions of complexity in forest management and silviculture. For Ecol Manage 421:59–71. https://doi.org/10.1016/j.foreco.2018.01.011

Fernández-Guisuraga JM, Calvo L, Suárez-Seoane S (2022) Monitoring post-fire neighborhood competition effects on pine saplings under different environmental conditions by means of UAV multispectral data and structure-from-motion photogrammetry. J Environ Manage 305:114373. https://doi.org/10.1016/j.jenvman.2021.114373

Fernández-Guisuraga JM, Suárez-Seoane S, Calvo L (2022) Radar and multispectral remote sensing data accurately estimate vegetation vertical structure diversity as a fire resilience indicator. Remote Sensing in Ecology and Conservation https://doi.org/10.1002/rse2.299

Gelman A, Goodrich B, Gabry J, Vehtari A (2019) R-squared for Bayesian Regression Models. Am Stat 73:307–309. https://doi.org/10.1080/00031305.2018.1549100

Germino MJ, Barnard DM, Davidson BE et al (2018a) Thresholds and hotspots for shrub restoration following a heterogeneous megafire. Landscape Ecol 33:1177–1194. https://doi.org/10.1007/s10980-018-0662-8

Germino MJ, Barnard DM, Davidson BE et al (2018b) Thresholds and hotspots for shrub restoration following a heterogeneous megafire. Landscape Ecol 33:1177–1194

Getzin S, Nuske RS, Wiegand K (2014) Using unmanned aerial vehicles (UAV) to quantify spatial gap patterns in forests. Remote Sensing 6:6988–7004

Girardeau-Montaut D (2016) CloudCompare. France: EDF R&D Telecom ParisTech, Stuttgart, Germany

Hijmans RJ, Bivand R, Forner K et al (2022) Package 'terra.' Vienna, Austria, Maintainer

Hobbs RJ, Huenneke LF (1992) Disturbance, Diversity, and Invasion: Implications for Conservation. Conserv Biol 6:324–337. https://doi.org/10.1046/j.1523-1739.1992.06030324.x

Hojatimalekshah A, Gongora J, Enterkine J et al (2023) Lidar and deep learning reveal forest structural controls on snowpack. Front Ecol Environ 21:49–54. https://doi.org/10.1002/fee.2584

Ilangakoon NT, Glenn NF, Dashti H et al (2018) Constraining plant functional types in a semi-arid ecosystem with waveform lidar. Remote Sens Environ 209:497–509. https://doi.org/10.1016/j.rse.2018.02.070

Ilangakoon N, Glenn NF, Schneider FD et al (2021) Airborne and Spaceborne Lidar Reveal Trends and Patterns of Functional Diversity in a Semi-Arid Ecosystem. Front Remote Sens 2:743320. https://doi.org/10.3389/frsen.2021.743320

Johnson DJ, Magee L, Pandit K et al (2021) Canopy tree density and species influence tree regeneration patterns and woody species diversity in a longleaf pine forest. For Ecol Manage 490:119082. https://doi.org/10.1016/j.foreco.2021.119082

Keitt TH, Fischer J (2006) Detection of Scale-Specific Community Dynamics Using Wavelets. Ecology 87:2895–2904. https://doi.org/10.1890/0012-9658(2006)87[2895:DOSCDU]2.0.CO;2

Koontz MJ, North MP, Werner CM et al (2020) Local forest structure variability increases resilience to wildfire in dry western U.S. coniferous forests. Ecol Lett 23:483–494. https://doi.org/10.1111/ele.13447

LaRue EA, Hardiman BS, Elliott JM, Fei S (2019) Structural diversity as a predictor of ecosystem function. Environ Res Lett 14:114011. https://doi.org/10.1088/1748-9326/ab49bb

Levin SA (1992) The Problem of Pattern and Scale in Ecology: The Robert H. MacArthur Award Lect Ecol 73:1943–1967. https://doi.org/10.2307/1941447

Lines ER, Fischer FJ, Owen HJF, Jucker T (2022) The shape of trees: Reimagining forest ecology in three dimensions with remote sensing. J Ecol 110:1730–1745. https://doi.org/10.1111/1365-2745.13944

Maestre FT, Eldridge DJ, Soliveres S et al (2016) Structure and functioning of dryland ecosystems in a changing world. Annu Rev Ecol Evol Syst 47:215–237. https://doi.org/10.1146/annurev-ecolsys-121415-032311

Maestre FT, Benito BM, Berdugo M et al (2021) Biogeography of global drylands. New Phytol 231:540–558. https://doi.org/10.1111/nph.17395

Mahood AL, Koontz MJ, Balch JK (2023) Fuel connectivity, burn severity, and seed bank survivorship drive ecosystem transformation in a semiarid shrubland. Ecology 104:e3968. https://doi.org/10.1002/ecy.3968

Marie V, Zaiats A, Roser A, et al (2023a) Digital aerial imagery (RGB and multispectral) from the 1996-COYOTE BUTTE wildfire boundary near Initial Point Kuna Idaho USA-2022. 46 GB. https://doi.org/10.7923/QXAV-S561

Marie V, Zaiats A, Roser A, et al (2023b) Digital aerial imagery (RGB and multispectral) from the 2007-COLD wildfire boundary near Glenns Ferry Idaho USA-2022. 96 GB. https://doi.org/10.7923/RAGG-TV25

Marie V, Zaiats A, Roser A, et al (2023c) Digital aerial imagery (RGB and multispectral) from the 2005-NORTH HAM wildfire boundary near Hammett Idaho USA-2022. 45 GB. https://doi.org/10.7923/2Q8W-SN16

Marie V, Zaiats A, Roser A, et al (2023d) Digital aerial imagery (RGB and multispectral) from within the lower Dry Creek watershed near Boise Idaho USA-2022. 64 GB. https://doi.org/10.7923/ZS2V-7B04

Marie V, Zaiats A, Roser A, et al (2023e) Digital aerial imagery (RGB and multispectral) from the 2013-PONY COMPLEX wildfire boundary near Mountain Home Idaho USA-2022. 100 GB. https://doi.org/10.7923/AEZG-KD35

Marie V, Zaiats A, Roser A, et al (2023f) Digital aerial imagery (RGB and multispectral) from the 2015-SODA wildfire boundary near the Oregon/Idaho border USA-2022. 85 GB. https://doi.org/10.7923/59M8-5S68.

Marie V, Zaiats A, Roser A, et al (2023g) Digital aerial imagery (RGB and multispectral) from the 2010-SOUTH TRAIL wildfire boundary near Hammett Idaho USA-2022. 56 GB. https://doi.org/10.7923/5JCE-YE15.

Meinke CW, Knick ST, Pyke DA (2009) A Spatial Model to Prioritize Sagebrush Landscapes in the Intermountain West (U.S.A.) for Restoration. Restor Ecol 17:652–659. https://doi.org/10.1111/j.1526-100X.2008.00400.x

Miller R, Chambers J, Pyke D et al (2013) A review of fire effects on vegetation and soils in the Great Basin region: response and site characteristics. Gen Tech Rep RMRS-GTR-308. Department of Agriculture, Forest Service. Fort

Collins, CO, USA. Available online: http://sagestep.org/pdfs/rmrs_gtr308.pdf. Accessed 18 May 2023

Nason G, Nason MG (2016) R Package 'wavethresh.' Available at https://cran.r-project.org/web/packages/wavethresh/wavethresh.pdf

Nimmo DG, Nally RM, Cunningham SC et al (2015) Vive la résistance: reviving resistance for 21st century conservation. Trends Ecol Evol 30:516–523. https://doi.org/10.1016/j.tree.2015.07.008

Pebesma EJ (2018) Simple features for R: standardized support for spatial vector data. R J 10:439

Piironen J, Vehtari A (2017) Sparsity information and regularization in the horseshoe and other shrinkage priors. Electron J Statist 11:. https://doi.org/10.1214/17-EJS1337SI

Pilliod DS, Jeffries MA, Welty JL, Arkle RS (2021) Protecting restoration investments from the cheatgrass-fire cycle in sagebrush steppe. Conservation Science and Practice 3:e508. https://doi.org/10.1111/csp2.508

Pyke DA, Knick ST, Chambers JC, et al (2015) Restoration handbook for sagebrush steppe ecosystems with emphasis on greater sage-grouse habitat-Part 2: Landscape level restoration decisions. Circular 1418 Washington, DC: US Department of the Interior; Reston, VA: US Geological Survey 43 p

R Core Team (2021) R: A Language and Environment for Statistical Computing. R Foundation for Statistical Computing, Vienna, Austria

Rayburn AP, Schiffers K, Schupp EW (2011) Use of precise spatial data for describing spatial patterns and plant interactions in a diverse Great Basin shrub community. Plant Ecol 212:585–594. https://doi.org/10.1007/s11258-010-9848-0

Reinhardt JR, Filippelli S, Falkowski M et al (2020) Quantifying Pinyon-Juniper Reduction within North America's Sagebrush Ecosystem. Rangel Ecol Manage. https://doi.org/10.1016/j.rama.2020.01.002

Requena-Mullor JM, Maguire KC, Shinneman DJ, Caughlin TT (2019) Integrating anthropogenic factors into regional-scale species distribution models—A novel application in the imperiled sagebrush biome. Glob Change Biol 25:3844–3858. https://doi.org/10.1111/gcb.14728

Retallack A, Finlayson G, Ostendorf B, Lewis M (2022) Using deep learning to detect an indicator arid shrub in ultra-high-resolution UAV imagery. Ecol Ind 145:109698. https://doi.org/10.1016/j.ecolind.2022.109698

Roberts CP, Donovan VM, Allen CR et al (2021) Monitoring for spatial regimes in rangelands. Rangel Ecol Manage 74:114–118. https://doi.org/10.1016/j.rama.2020.09.002

Roussel J-R, Auty D, Coops NC et al (2020) lidR: An R package for analysis of Airborne Laser Scanning (ALS) data. Remote Sens Environ 251:112061. https://doi.org/10.1016/j.rse.2020.112061

Schwinning S, Weiner J (1998) Mechanisms determining the degree of size asymmetry in competition among plants. Oecologia 113:447–455. https://doi.org/10.1007/s004420050397

Seidel D, Ehbrecht M, Annighöfer P, Ammer C (2019) From tree to stand-level structural complexity — Which properties make a forest stand complex? Agric for Meteorol 278:107699. https://doi.org/10.1016/j.agrformet.2019.107699

Shriver RK, Andrews CM, Arkle RS et al (2019) Transient population dynamics impede restoration and may promote ecosystem transformation after disturbance. Ecol Lett 22:1357–1366. https://doi.org/10.1111/ele.13291

Simler-Williamson AB, Applestein C, Germino MJ (2022) Interannual variation in climate contributes to contingency in post-fire restoration outcomes in seeded sagebrush steppe. Conservation Science and Practice e12737. https://doi.org/10.1111/csp2.12737

Smith JT, Allred BW, Boyd CS et al (2021) Where there's smoke, there's fuel: predicting Great Basin rangeland wildfire. Biorxiv. https://doi.org/10.1101/2021.06.25.449963

Spake R, Mori AS, Beckmann M et al (2021) Implications of scale dependence for cross-study syntheses of biodiversity differences. Ecol Lett 24:374–390. https://doi.org/10.1111/ele.13641

Spake R, Barajas-Barbosa MP, Blowes SA et al (2022) Detecting Thresholds of Ecological Change in the Anthropocene. Annu Rev Environ Resour 47:797–821. https://doi.org/10.1146/annurev-environ-112420-015910

Spiers A, Scholl V, McGlinchy J et al (2021) UAS for forest inventory traits: a review. EcoEvoRxiv. https://doi.org/10.32942/osf.io/xjdt3

Standish RJ, Hobbs RJ, Mayfield MM et al (2014) Resilience in ecology: Abstraction, distraction, or where the action is? Biol Cons 177:43–51. https://doi.org/10.1016/j.biocon.2014.06.008

Strand EK, Robinson AP, Bunting SC (2007) Spatial patterns on the sagebrush steppe/Western juniper ecotone. Plant Ecol 190:159–173. https://doi.org/10.1007/s11258-006-9198-0

Suding KN, Gross KL, Houseman GR (2004) Alternative states and positive feedbacks in restoration ecology. Trends Ecol Evol 19:46–53. https://doi.org/10.1016/j.tree.2003.10.005

Walter JA, Sheppard LW, Anderson TL et al (2017) The geography of spatial synchrony. Ecol Lett 20:801–814. https://doi.org/10.1111/ele.12782

Walter JA, Stovall AEL, Atkins JW (2021) Vegetation structural complexity and biodiversity in the Great Smoky Mountains. Ecosphere 12:e03390. https://doi.org/10.1002/ecs2.3390

Webb NP, McCord SE, Edwards BL et al (2021) Vegetation Canopy Gap Size and Height: Critical Indicators for Wind Erosion Monitoring and Management. Rangel Ecol Manage 76:78–83. https://doi.org/10.1016/j.rama.2021.02.003

Welty J, Jeffries M (2021) Combined wildland fire datasets for the United States and certain territories, 1800s-Present. U.S. Geological survey data release. Available at: https://doi.org/10.5066/P9ZXGFY3

White PS, Walker JL (1997) Approximating Nature's Variation: Selecting and Using Reference Information in Restoration Ecology. Restor Ecol 5:338–349. https://doi.org/10.1046/j.1526-100X.1997.00547.x

Wickham H (2011) ggplot2. Wiley Interdiscip Rev: Comput Stat 3:180–185

Wickham H, Averick M, Bryan J et al (2019) Welcome to the Tidyverse. J Open Sourc Software 4:1686

Willim K, Stiers M, Annighöfer P et al (2020) Spatial Patterns of Structural Complexity in Differently Managed and

Unmanaged Beech-Dominated Forests in Central Europe. Remote Sens 12:1907. https://doi.org/10.3390/rs121 21907

Wu J (2004) Effects of changing scale on landscape pattern analysis: scaling relations. Landscape Ecol 19:125–138. https://doi.org/10.1023/B:LAND.0000021711.40074.ae

Zahawi RA, Dandois JP, Holl KD et al (2015) Using lightweight unmanned aerial vehicles to monitor tropical forest recovery. Biol Cons 186:287–295

Zaiats A, Cattau ME, Pilliod DS et al (2023) Forecasting natural regeneration of sagebrush after wildfires using population models and spatial matching. Landsc Ecol. https://doi.org/10.1007/s10980-023-01621-1

Zhang W, Qi J, Wan P et al (2016) An easy-to-use airborne LiDAR data filtering method based on cloth simulation. Remote Sens 8:501

Zhao Y, Ogden RT, Reiss PT (2012) Wavelet-Based LASSO in Functional Linear Regression. J Comput Graph Stat 21:600–617. https://doi.org/10.1080/10618600.2012.679241

Zhao Y, Chen H, Ogden RT (2015) Wavelet-Based Weighted LASSO and Screening Approaches in Functional Linear Regression. J Comput Graph Stat 24:655–675

Ziegenhagen LL, Miller RF (2009) Postfire Recovery of Two Shrubs in the Interiors of Large Burns in the Intermountain West, USA. wnan 69:195–205. https://doi.org/10.3398/064.069.0208